journal

J. Am. Ceram. Soc., 90 [4] 1101–1106 (2007)
DOI: 10.1111/j.1551-2916.2007.01533.x

PMN–PT Ceramics Prepared By Spark Plasma Sintering

Ruzhong Zuo,† Torsten Granzow, Doru C. Lupascu, and Jürgen Rödel

Institute of Materials Science, Darmstadt University of Technology, Petersenstr. 23, Darmstadt, Germany

$(1-x)Pb(Mg_{1/2}Nb_{2/3})O_3-xPbTiO_3$ (PMN–PT) ceramics of stoichiometric composition were fabricated by conventional pressureless sintering (CS) and spark plasma sintering (SPS). The CS ceramics exhibited a change from relaxor to normal ferroelectric behavior (FE) with increasing PT content. However, low dielectric constants, frequency dispersion, and diffuse phase transition behavior typical for relaxors were obtained for all SPS ceramics. FE and piezoelectric measurements further demonstrated low remanent polarization and strain, high coercive field, and low electromechanical response from SPS materials. Normal dielectric and enhanced FE performance appeared following high-temperature heat treatment after SPS. The effects of grain size, microstructure, and chemical heterogeneity formed during fast sintering are considered.

I. Introduction

Lead magnesium niobate $Pb(Mg_{1/3}Nb_{2/3})O_3$ (PMN) belongs to the lead-containing complex perovskite family with a general formula $Pb(B_1,B_2)O_3$. Many members of this family are typical relaxor ferroelectrics (FE), showing broad diffuse dielectric maxima at the transition from the FE to the paraelectric (PE) phase and frequency-dispersive permittivity versus temperature curves.[1–4] These typical properties of relaxor FEs are attributed to the breakdown of the FE long-range order and the appearance of small polar regions, often referred to as nanodomains or polar clusters, at high temperatures. With increasing temperature, the size of these nanodomains decreases and their mobility increases, until they can no longer be evidenced. The existence of nanodomains is generally considered to be closely linked to internal electric fields in the material. One reason for the appearance of these fields is the local heterogeneity of the sample composition.

PMN forms solid solutions with a normal FE lead titanate $PbTiO_3$ (PT), with a reported morphotropic phase boundary (MPB) in the composition range of 32–35 mol% PT where the materials exhibit high-dielectric and piezoelectric properties.[5,6] With increasing PT content, these solid solutions of PMN–PT undergo a gradual transition from a relaxor to a normal FE, which has an abrupt dielectric peak near the Curie temperature (T_c). It was reported that single crystals or polycrystalline PMN–PT with a grain size of 8–9 μm of MPB compositions exhibit a normal FE transition.[7,8] It has also been found that the dielectric constant in PMN-based materials is grain size dependent and increases with increasing grain size.[9–11] The relative role of extrinsic mechanisms, like domain wall motion, in piezoelectric properties was deduced to be influenced strongly by grain size.[12]

PMN–PT ceramics have been manufactured in different ways,[13–18] including conventional pressureless sintering (CS), microwave sintering, hot pressing, hot-isostatic pressing (HIP), etc. These techniques lead to different densification behavior and microstructures. It is well-known that the grain size and porosity play a fundamental role in the dielectric and electromechanical response.[19] When trying to control these parameters, spark plasma sintering (SPS) is a useful tool. It is a fast densification process that utilizes microscopic electrical discharges between particles under pressure. It allows sintering of a powder compact to a high density at relatively low temperatures and within much shorter sintering periods. The short sintering time for the SPS process could be advantageous in suppressing grain growth and lead loss typical of sintering lead-containing perovskite FEs. Although SPS is commonly used to produce dense metal and engineering ceramics, attempts to prepare dielectric, FE, and piezoelectric ceramics with fine grain sizes by this technique have only been made in recent years.[20–27] The results show that the SPS samples exhibit enhanced permittivity, increased coercive field, and a diffuse PE/FE transition, in contrast to the CS ones.

However, this novel process was rarely applied to sinter PMN–PT ceramics, although its short processing time and low temperature may aid PMN–PT preparation by reducing lead loss, improving density, etc. Our purpose is to investigate whether SPS can be used to sinter PMN–PT, and how the properties can be influenced. For comparison, the powders of the same compositions were also sintered by a CS process. A significant difference in properties concerning remnant polarization (P_r), maximum strain (S_m), and dielectric constant (K) was found between the SPS and CS samples. Abnormal electrical properties in SPS samples are correlated to the changes in grain size, microstructure, and chemical homogenization. These findings should contribute to a better understanding of the correlations between the FE properties of PMN–PT ceramics and the processing.

II. Experimental Procedure

(1) Sample Preparation

The starting materials for the samples used in this study were PbO (>99.0%, Alfa Aesar, Karlsruhe, Germany), $MgCO_3 \cdot Mg(OH)_2 \cdot 6H_2O$ (99.5%, Alfa Aesar), Nb_2O_5 (99.9%, ChemPur, Germany), and TiO_2 (99.9%, Alfa Aesar). The columbite precusor[28] method was used to prepare $(1-x)Pb(Mg_{1/2}Nb_{2/3})O_3-xPbTiO_3$ powders ($x = 0.25$, 0.32, and 0.4) that are near the MPB. The columbite, $MgNb_2O_6$ (MN), was synthesized by attrition milling $MgCO_3 \cdot Mg(OH)_2 \cdot 6H_2O$ and Nb_2O_5 for 12 h, followed by calcination at 1200°C for 4 h. The dried MN powder, PbO, and TiO_2 were weighed according to the stoichiometric formula and ball milled in ethanol for 24 h with a planetary mill and yttrium-stabilized zirconia balls, 5 and 10 mm in diameter. The mixed powder was then calcined in an alumina crucible at 850°C for 2 h. After calcination, the powder was further ground for 24 h using the above-mentioned planetary ball mill. Pellets 10 mm in diameter and 3 mm in thickness for the CS process were uniaxially pressed at 50 MPa in a stainless-steel die.

PMN–PT samples were sintered by two methods for comparison (1) CS at 1200°C for 4 h at a heating rate of 5°C/min in a tube furnace (GERO Hochtemperaturöfen GmbH, Neuhausen, Germany). The pellets were covered with the powder of the same composition, and (2) SPS at 950°C for 2 min under a uniaxial pressure of 50 MPa in an SPS equipment (Dr. Sinter 2050,

D. Viehland—contributing editor

Manuscript No. 22149. Received August 24, 2006; approved November 28, 2006.
This work was financially supported by the Deutsche Forschungsgemeinschaft (SFB 595).
†Author to whom correspondence should be addressed. email: zuo@ceramics.tu-darmstadt.de

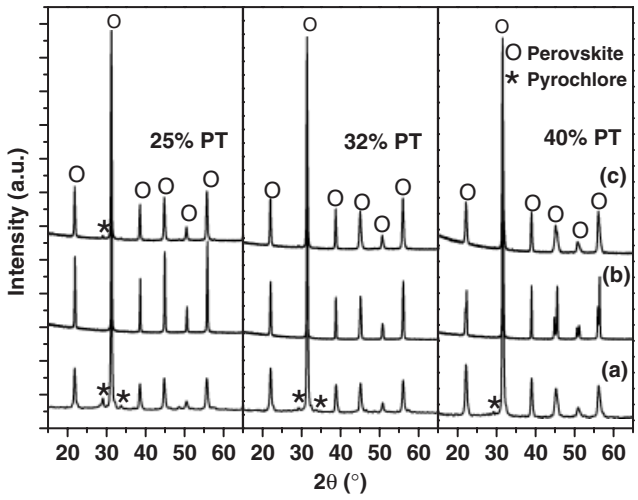

Fig. 1. XRD patterns for three PMN–PT compositions: (a) calcined powders at 850°C for 2 h, (b) CS-sintered samples at 1200°C for 4 h, and (c) SPS samples sintered at 950°C for 2 min. PMN, lead magnesium niobate; PT, lead titanate; CS, conventional pressureless sintering; SPS, spark plasma sintering; XRD, X-ray diffraction.

Sumitomo Coal Ming Co., Tokyo, Japan) equipped with a graphite die 12 mm in inner diameter through which a pulsed direct current can pass. The heating and cooling rates are 100°C/min and 500°C/min, respectively. In the case of SPS, samples were reoxidized through oxidation in air at 550°C for 10 h. Some of the SPS samples were annealed at 1000°C for 6 h and 1150°C for 10 h, respectively, again covered with the powder of the same composition to minimize the loss of PbO.

(2) Characterization

The density of the sintered samples was measured by the Archimedes method. Powder X-ray diffraction (XRD, STOE, Darmstadt, Germany) patterns of crushed CS and SPS pellets and calcined powders were recorded in the 2θ range of 15°–65°. The microstructure of the sintered samples was observed on fracture surfaces by means of high-resolution scanning electron microscopy (HR-SEM, Model No. XL 30 FEG, Philips Electronic Instruments, Mahwah, NJ). The particle size of the as-prepared powder was estimated to be ~650 nm using HR-SEM.

For the dielectric and piezoelectric measurements, silver electrodes were pasted on both sides of the polished sample disks and fired at 750°C for 30 min. The temperature and frequency dependence of the dielectric constants was measured using a computer-controlled LCR meter (Mode: HP4284A, Hewlett-Packard, Palo Alto, CA) in the frequency range from 100 Hz to 1 MHz and a temperature range of 30°–300°C. Specimens for the piezoelectric measurement were poled at 100°C in a stirred silicone oil bath by applying a dc electric field of 3 kV/mm for 30 min, and then cooled to room temperature while maintaining the electric field. The planar electromechanical coupling factor k_p was obtained by a resonance–antiresonance method through an impedance analyzer (Mode: HP 4192A, Hewlett-Packard, Palo Alto, CA) on the basis of IEEE standards.[29] The sample disks for k_p measurement had an aspect ratio of at least 10. The piezoelectric coefficient d_{33} was measured 24 h after poling by a quasi-static Belincourt-meter (Model YE2730 SINOCERA, Shanghai, China). Polarization and strain hysteresis loops of unpoled samples were measured in a silicone oil bath by applying an electric field of triangular waveform with an amplitude of 3 kV/mm and a frequency of 50 mHz.

III. Results And Discussion

XRD for three compositions of PMN–PT solid solutions are shown in Fig. 1. The crystal structure changes from rhombohedral to tetragonal with increasing PT content. It is well-known that the composition of 32% PT for PMN–PT solid solution systems lies at the MPB.[5,6] A small amount of secondary phase, pyrochlore, still exists just after calcination. The pyrochlore phase was absent after the samples were sintered at 1200°C. The SPS PMN–25%PT still contained some, as it was sintered

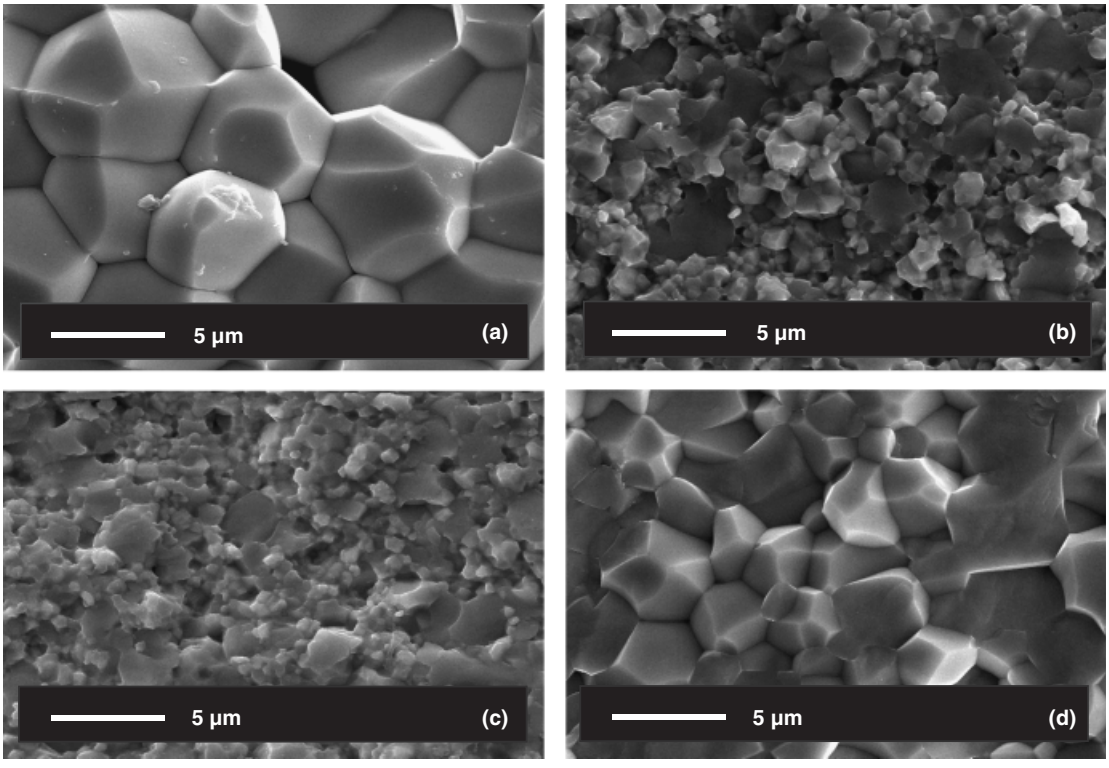

Fig. 2. SEM pictures on fracture surfaces of PMN–32PT ceramics: (a) CS sample sintered at 1200°C for 4 h, (b) SPS sample sintered at 950°C for 2 min, (c) thermally treated SPS PMN–32%PT sample at 1000°C for 6 h, and (d) thermally treated SPS PMN–32%PT sample at 1150°C for 10 h. PMN, lead magnesium niobate; PT, lead titanate; CS, conventional pressureless sintering; SPS, spark plasma sintering; SEM, scanning electron microscopy.

Table I. Room-Temperature Dielectric Properties and Piezoelectric Responses of CS and SPS PMN–PT Solid Solution Ceramics

Compositions	PMN–25%PT		PMN–32%PT		PMN–40%PT	
Sintering processing	CS	SPS	CS	SPS	CS	SPS
Density (%)	98.5	99.5	98.0	99.3	98.3	99.1
Type of phase transition	Relaxor	Relaxor	Normal	Relaxor-like	Normal	Relaxor-like
Coupling factor k_p (%)	42	19	57	33	40	25
Piezoelectric strain coefficient d_{33} (pC/N)	315	101	336	185	235	145
d_{33} after heat-treatment at 1150°C for 10 h	—	300	—	350	—	228

PMN, lead magnesium niobate; PT, lead titanate; CS, conventional pressureless sintering; SPS, spark plasma sintering.

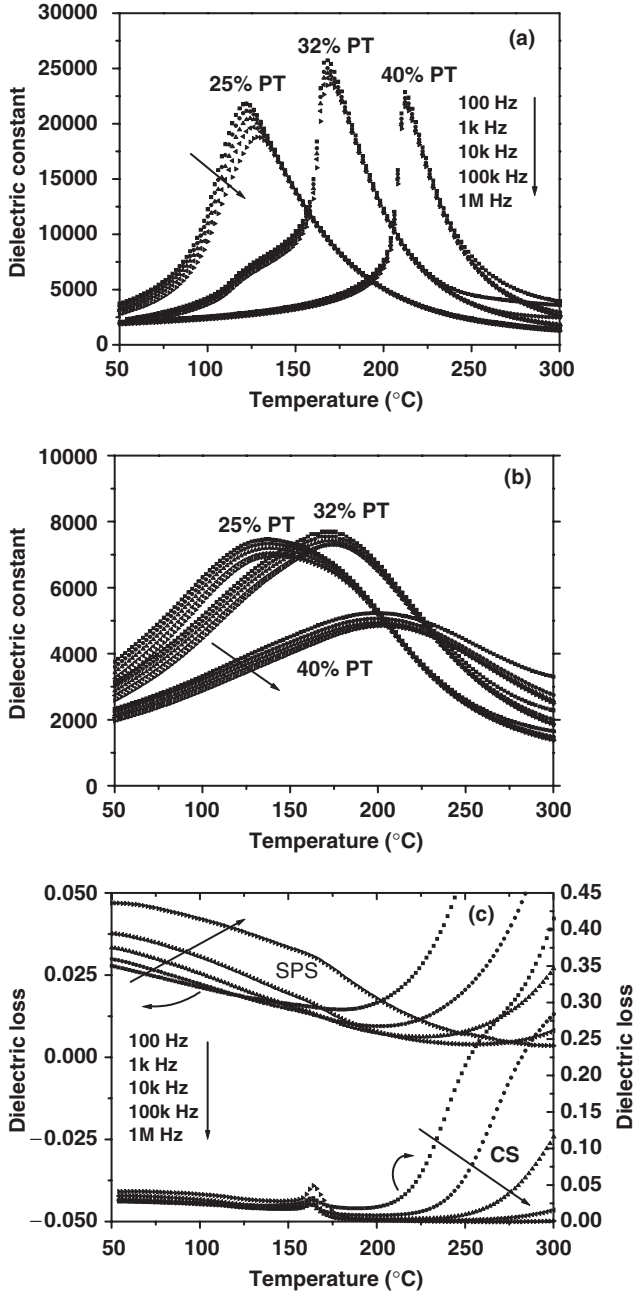

Fig. 3. Temperature and frequency dependence of the dielectric constants for PMN–PT ceramics with three different PT contents prepared by (a) CS and (b) SPS, respectively, and (c) the dielectric losses for CS and SPS PMN–32%PT ceramics. PMN, lead magnesium niobate; PT, lead titanate; CS, conventional pressureless sintering; SPS, spark plasma sintering.

at a low temperature. Moreover, the calcined powder of PMN–40%PT shows a rhombohedral, not a tetragonal structure, although it is far away from the MPB. The tetragonal phase was formed for the samples after sintering at 1200°C. The SPS samples show structures similar to those of the calcined powders of the same composition. This could be attributed to the particle size effect of the crystal structure, as the calcined powder after milling and the SPS sample have fine particle (grain) sizes. This effect was also observed in SPS and HIP fine-grained $BaTiO_3$ ceramics,[30,31] where it was pointed out that when the grain size of $BaTiO_3$ decreases below a few micrometers, the crystallographic cell becomes less and less tetragonal and the fraction of the cubic phase increases.

As an example, Fig. 2 compares the microstructures of the CS and SPS PMN–32%PT samples. The microstructure of the SPS samples after annealing at 1000°C for 6 h and 1150°C for 10 h is also included. It shows that fast sintering, i.e., a short densification process, leads to microstructure inhomogeneity and very small grains. The grain size is about eight times larger for CS samples (~7 μm in average) than SPS samples (~0.8 μm in average). The heat treatment of the SPS samples at 1000°C did not significantly change the microstructure, although the compositional fluctuation that occurs during fast sintering can be improved. However, the grains start to grow to the same level as in the CS samples and become homogenous after re-firing at 1150°C. The same features were observed in the samples of other compositions. The density of each sample is given in Table I. The SPS samples show a higher density than the CS samples, as measured using the Archimedes method. All samples have densities of more than 98% of the theoretical density.

Dielectric constants were measured as a function of temperature and frequency for samples of different compositions, as shown in Figs. 3(a) and (b). Frequency-dependent dielectric properties and diffuse phase transition (DPT) characteristics were observed for samples with 25% PT, which is typical of relaxors. At 40% PT, the samples appear to be normal ferroelectrics, showing a sharp phase transition. PMN–32%PT ceramics also exhibit normal PE/FE transition. In addition, a second transition exists at about 120°C, which is due to a transition from a rhombohedral to a tetragonal structure according to the phase diagram.[32,33] This transition indicates frequency dispersion. The existence of the second phase transition further implies that the MPB of PMN–PT solid solutions lies close to 32% PT. In contrast to this, the SPS samples of all compositions show DPT and frequency-dispersive dielectric properties. With increasing frequency, the dielectric maxima (K_{max}) are shifted to a higher temperature and lower values. By comparison, K_{max} for all SPS samples were lower than those of the CS samples. The degraded dielectric permittivity may be related to the increasing percentage of PbO-rich grain-boundary phases. It is known that the smaller the grain size of the samples, the higher the fraction of grain-boundary phase. Moreover, it was suggested that local heterogeneity in composition or microstructure contributes to DPT and frequency dependence of the dielectric properties.[15] This usually exists in such complex B-site or A-site perovskite structures as $Pb(Mg_{1/2}Nb_{2/3})O_3$ and $(PbLa)(ZrTi)O_3$, etc.[34–36] It was confirmed that the columbite process for making PMN–PT powder can result in a non-uniform distribution of constituent elements during the formation of the powder.[15] This chemical

heterogeneity remained after SPS to full density due to lack of sufficient chemical diffusion during fast sintering. This kind of heterogeneity, which was also examined in hot-pressed PMN–35%PT ceramics,[15] can also contribute to the relaxor-like behavior of the SPS PMN–PT ceramics. Even for the PMN–25%PT composition, which is intrinsically a relaxor, the SPS sample of this composition exhibits a more DPT and a stronger frequency dependence of the dielectric constant. From the dielectric losses (Fig. 3(c)), it can also be seen that SPS PMN–32%PT shows diffuse and frequency-dependent dielectric properties; however, the values for SPS samples are close to those for CS samples below the Curie temperature.

The remanent polarization P_r and strain S versus electric field are shown in Fig. 4. It can be seen that the PMN–32%PT ceramic exhibits stronger ferroelectricity, showing larger P_r and S_m. It is well-known that MPB compositions have superior FE and piezoelectric properties. Owing to the co-existence of different phases, the polar axis of each grain can take more spatial orientations and thus align more easily along the direction of the external electric field.[37–39] Compared with the CS samples, the values of P_r were rather low and the coercive field (E_c) rather high in all SPS samples. P_r and E_c are 27.0 μC/cm^2 and 0.36 kV/mm, respectively, for the CS PMN–32%PT; however, the SPS counterpart has a P_r and an E_c of 16.5 μC/cm^2 and 0.56 kV/mm. The P–E curves become thinner for SPS samples. The CS samples show more butterfly-like hysteretic strain curves than all SPS samples, which show the behavior typical of relaxors. The increase of E_c and the decrease of P_r for SPS samples could be related to the fine grain morphology, as shown in Fig. 2. Fine-grained ceramics usually have a larger grain boundary phase fraction, which would obstruct domain wall movement under an external electric field and also lower the effective electric field on each grain.[40,41] This could also cause a low strain value produced under the same external electric field. The explanation can be supported by annealing the SPS samples under sufficient temperature and time conditions. Fig. 5 shows the measurement of P and S versus electric field for the annealed SPS PMN–32%PT samples. After the sample was heated to 1000°C for 6 h, the FE polarization and strain values showed little difference from those of the original SPS samples of the same composition. However, when the sample was heated to 1150°C for 10 h, FE behavior similar to that of the CS samples emerged. This can be seen by a comparison of Figs. 4 and 5. As can be seen from Fig. 2, the microstructure was not changed by heat treatment at 1000°C for 6 h and the average grain size is about 0.87 μm. However, it became similar to that of the CS sample after heat treatment at 1150°C for 10 h. The average grain size is about 6 μm. Grain growth and homogenization of the compositional distribution through high-temperature heat treatment could be the reason for the increase of the FE properties of the SPS samples. Additionally, the dielectric properties were also changed for the same reason. The frequency and temperature dependency of the dielectric constants of annealed SPS PMN–32%PT ceramics are shown in Fig. 6. The SPS samples annealed at 1000°C show less frequency dispersion, due to the improvement of chemical homogenization. The fine grain size still remains after heat treatment (Fig. 2(c)) and causes the broad DPT and low dielectric maxima. The SPS PMN–32%PT annealed at 1150°C still has lower dielectric maxima than the CS counterpart, probably because the grain size remains smaller, and lead loss increases during annealing. However, the DPT and frequency dispersion disappeared at the FE phase transition. Based on this, the CS PMN–32%PT and PMN–40%PT ceramics show no DPT characteristic, but normal FE phase transitions. For this processing, the chemical heterogeneity of the as-prepared powder was eliminated by long-term high-temperature sintering. Therefore, two distinct effects in SPS PMN–PT samples contribute to the FE and dielecric properties: grain size and heterogeneity in composition and chemistry. The grain size effect (in the size range of our study) is suggested to be responsible for lowering the dielectric maxima and apparent ferroelectricity, and the heterogeneity contributes to the relaxor-like behavior of

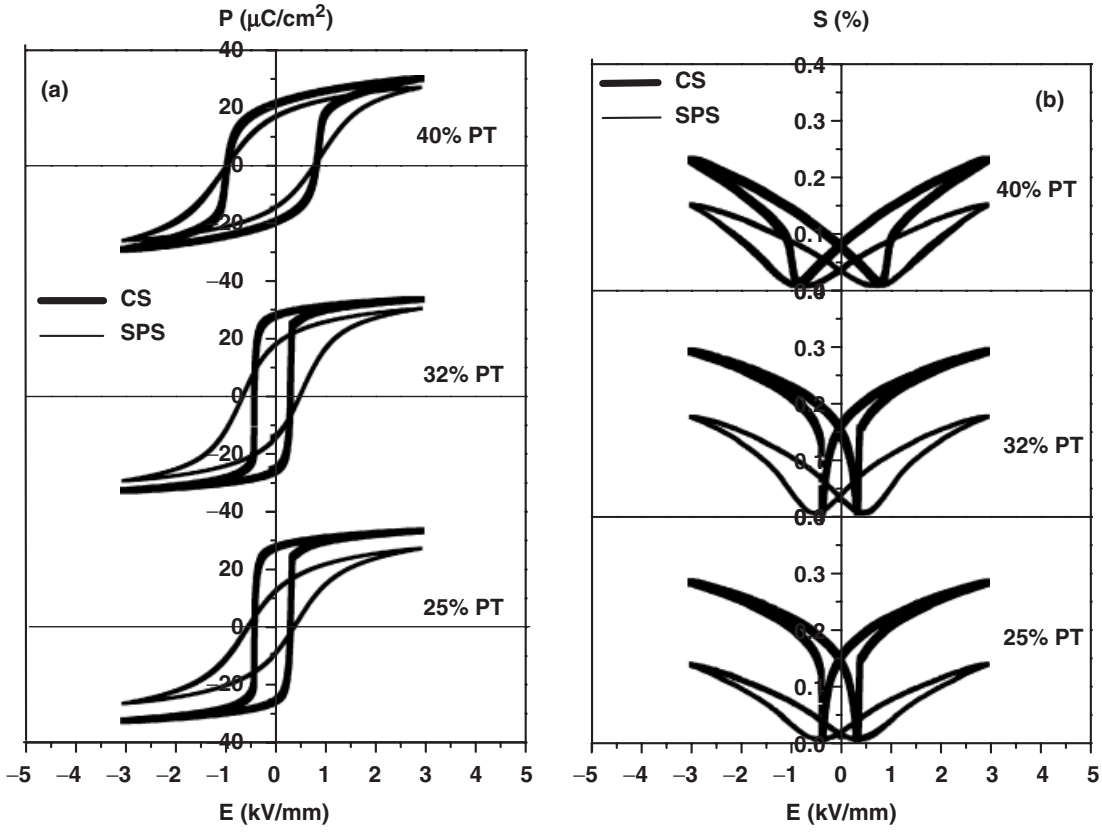

Fig. 4. Polarization (a) and strain (b) hysteresis loops of three PMN–PT ceramics sintered by CS and SPS processing. PMN, lead magnesium niobate; PT, lead titanate; CS, conventional pressureless sintering; SPS, spark plasma sintering.

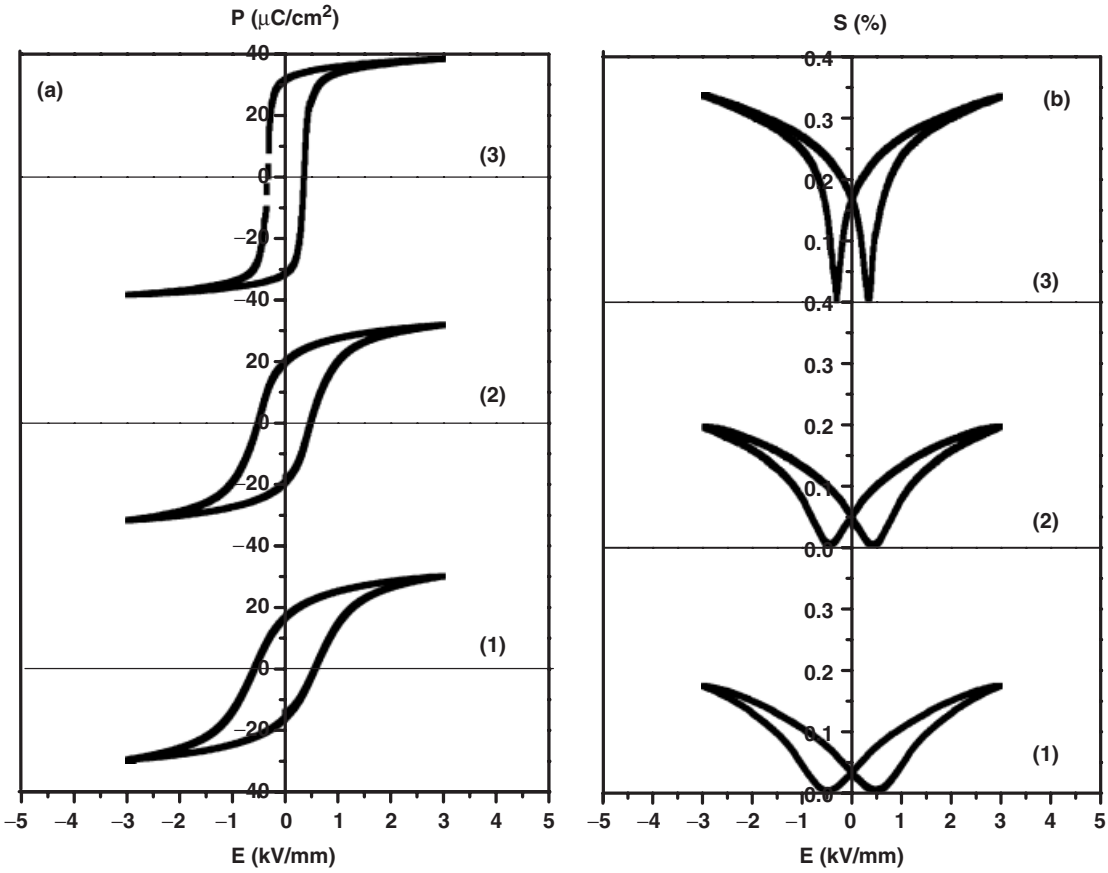

Fig. 5. Polarization (a) and strain (b) hysteresis loops of SPS PMN–32%PT ceramic samples: (1) virgin SPS samples, (2) heat-treated at 1000°C for 6 h, and (3) processed by heat treatment at 1150°C for 10 h. PMN, lead magnesium niobate; PT, lead titanate; SPS, spark plasma sintering.

the SPS samples. The correlations between electrical properties such as relaxor behavior and grain size, domain size, and pattern were investigated in perovskite ceramics.[42–44] With increasing PT content, PMN–PT ceramics either have domain patterns from polar nanodomains to tweed-like domains and finally to normal micrometer-sized domains,[42] or relaxation can be driven in normal FC PMN–35%PT and $BaTiO_3$ by reducing the grain size to the range of 100 nm, even smaller.[43,44] The relaxor response was considered attributable to the nanometer domains that contain a 1:1 short-range ordering on the B-site sublattice. This is similar to the compositional fluctuation on the nanoscale.

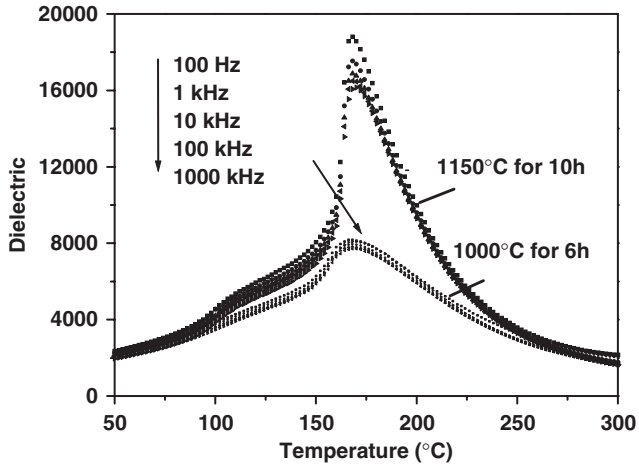

Fig. 6. Temperature and frequency dependence of the dielectric constants for SPS PMN–32%PT ceramics after different heat treatments (see inset). PMN, lead magnesium niobate; PT, lead titanate; SPS, spark plasma sintering.

Grain size changes the domain patterns under the condition that it is very small. Such a grain size effect on relaxor behavior was never seen in submicrometer-scaled PMN–PT samples, particularly larger than 700 nm in our cases.

The piezoelectric properties of PMN–PT ceramic samples are also shown in Table I. As expected, the MPB composition of PMN–PT solid solutions exhibited better electromechanical performance. The SPS samples show lower piezoelectric strain coefficients d_{33} and electromechanical coupling factors k_p than their CS counterparts, although the former have a much higher density. This is consistent with the measurement of dielectric and FE properties stated above. After thermal treatment, the SPS samples show an enhanced electromechanical coupling response close to that of the CS samples. The measurement of dielectric properties shows normal permittivity versus temperature and frequency response for SPS samples, except for the PMN–25%PT composition, which is intrinsically a relaxor. Some cases of a low electromechanical response and relaxor-like FE behavior of SPS electroceramics have been reported in the literature.[45,46] However, the enhanced permittivity by SPS was not found in our study on PMN–PT ceramics. The possible reason could be that PMN-based materials are intrinsically relaxors, based on the B-site complex occupation. Fast sintering for SPS processing tends to cause micro- or macro-inhomogenity, inducing relaxor-like FE behavior.

IV. Conclusions

Compared with conventional pressureless sintering, SPS demonstrates superior efficiency in densifying PMN–PT ceramics. PMN–PT solid solution ceramics show a transition from relaxor to normal FE behavior. However, a strongly frequency dependent and broad DPT was observed for all SPS samples, together with low remanent polarization and strain, and a high coercive

field. These exceptional electrical properties of SPS samples are attributed to the fine grain size and the heterogeneity in microstructure and composition.

Acknowledgments

We thank Z. Zhao from Stockholm University for his SPS experimental support; Mark Hoffman from The University of New South Wales for helpful discussion.

References

[1]S. Nomura and K. Uchino, "Electrostrictive Effect in $Pb(Mg_{1/3}Nb_{2/3})O_3$-Type Materials," *Ferroelectrics*, **41** [1–4] 251–66 (1982).
[2]L. E. Cross, "Relaxor Ferroelectrics," *Ferroelectrics*, **76** [3–4] 241–67 (1987).
[3]K. Uchino, "Relaxor Ferroelectrics," *J. Ceram. Soc. Jpn.*, **99** [10] 829–35 (1991).
[4]J. H. Park, B. K. Kim, and S. J. Park, "Electrostrictive Coefficients of 0.9Pb(Mg1/3Nb2/3)O-3-O.1PbTiO(3) Relaxor Ferroelectric Ceramics in the Ferroelectricity-Dominated Temperature Range," *J. Am. Ceram. Soc.*, **79** [2] 430–4 (1996).
[5]J. C. Ho, K. S. Liu, and I. N. Lin, "Study of Ferroelectricity in the PMN–PT System Near the Morphotropic Phase Boundary," *J. Mater. Sci.*, **28** [16] 4497–502 (1993).
[6]J. Kelly, M. Leonard, and C. Tantigate *et al.*, "Effect of Composition on the Electromechanical Properties of $(1-x)Pb(Mg_{1/3}Nb_{2/3})O_3-xPbTiO_3$ Ceramics," *J. Am. Ceram. Soc.*, **80** [4] 957–64 (1997).
[7]T. R. Shrout, Z. P. Chang, N. Kim, and S. Markgraf, "Dielectric Behavior of Single Crystals Near the $(1-x)Pb(Mg_{1/3}Nb_{2/3})O_3-xPbTiO_3$ Morphotropic Phase Boundary," *Ferroelectr. Lett.*, **12** [3] 63–9 (1990).
[8]S. M. Gupta and D. Viehland, "Tetragonal to Rhombohedral Transformation in the Lead Zirconium Titanate Lead Magnesium Niobate Lead Titanate Crystalline Solution," *J. Appl. Phys.*, **83** [1] 407–14 (1998).
[9]P. Papet, J. P. Dougherty, and T. R. Shrout, "Particle and Grain Size Effects on the Dielectric Behavior of the Relaxor Ferroelectric $Pb(Mg_{1/3}Nb_{2/3})O_3$," *J. Mater. Res.*, **5** [12] 2902–9 (1990).
[10]C. A. Randall, A. D. Hilton, D. J. Barber, and T. R. Shrout, "Extrinsic Contributions to the Grain Size Dependence of Relaxor Ferroelectric $(Pb(Mg_{1/3}Nb_{2/3})O_3$–$PbTiO_3$ Ceramics," *J. Mater. Res.*, **8** [4] 880–4 (1993).
[11]T. R. Shrout, U. Kumar, M. Megherhi, and N. Yang, "Grain Size Dependence of Dielectric and Electrostriction of $Pb(Mg_{1/3}Nb_{2/3})O_3$ Based Ceramics," *Ferroelectrics*, **76** [3–4] 479–87 (1987).
[12]C. A. Randall, N. Kim, J. P. Kucera, W. Cao, and T. R. Shrout, "Intrinsic and Extrinsic Size Effects in Fine-Grained Morphotropic-Phase-Boundary Lead Zirconate Titanate Ceramics," *J. Am. Ceram. Soc.*, **81** [3] 677–88 (1998).
[13]Z. P. Xie, Z. L. Gui, L. T. Li, T. Su, and Y. Huang, "Microwave Sintering of Lead-Based Relaxor Ferroelectric Ceramics," *Mater. Lett.*, **36** [1–4] 191–4 (1998).
[14]H. Yamada, "Pressureless Sintering of PMN-PT Ceramics," *J. Euro. Ceram. Soc.*, **19** [6–7] 1053–6 (1999).
[15]Z. Surowiak, M. F. Kupriyanov, A. E. Panich, and R. Skulski, "The Properties of the Non-Stoichiometric Ceramics $(1-x)Pb(Mg_{1/3}Nb_{2/3})O_3$–$(x)PbTiO_3$," *J. Euro. Ceram. Soc.*, **21** [15] 2783–6 (2001).
[16]E. R. Leite, "Chemical Heterogeneity in PMN–35PT Ceramics and Effects on Dielectric and Piezoelectric Properties," *J. Am. Ceram. Soc.*, **85** [12] 3018–24 (2002).
[17]M. H. Lente, A. L. Zanin, S. B. Assis, I. A. Santos, J. A. Eiras, and D. Garcia, "Effect of the Composition and Sintering Process on the Electrical Properties in $Pb(Mg_{1/3}Nb_{2/3})O_3$–$PbTiO_3$ Ceramics," *J. Euro. Ceram. Soc.*, **24** [6] 1529–33 (2004).
[18]M. R. Cox, "Large Diameter High Performance PMN–PT 90/10 Ceramic Produced by Hot Pressing," *J. Mater. Sci. Lett.*, **19** [4] 333–4 (2000).
[19]K. Okazaki and K. Nagata, "Effects of Grain Size and Porosity on Electrical and Optical Properties of PLZT Ceramics," *J. Am. Ceram. Soc.*, **56** [4] 82–6 (1973).
[20]A. Onodera, K. Yoshio, H. Satoh, H. Yamashita, and N. Sakagami, "Li-Substitution Effect and Ferroelectric Properties in Piezoelectric Semiconductor ZnO," *Jpn. J. Appl. Phys.*, **37** [4 Part 1] 5315–7 (1998).
[21]T. Takeuchi, E. Betourne, M. Tabuchi, H. Kageyama, Y. Kobayashi, A. Coats, F. Morrison, D. Sinclair, and A. West, "Dielectric Properties of Spark-Plasma-Sintered $BaTiO_3$," *J. Mater. Sci.*, **34** [5] 917–24 (1999).
[22]G. Zhan, J. Kuntz, J. Wan, J. Garay, and A. Mukherjee, "Spark-plasma-sintered $BaTiO_3/Al_2O_3$ Nanocomposites," *Mater. Sci. Eng.*, **A356** [1–2] 443–6 (2003).
[23]T. Takeuchi, M. Tabuchi, I. Kondoh, N. Tamari, and H. Kageyama, "Synthesis of Dense Lead Titanate Ceramics with Submicrometer Grains by Spark Plasma Sintering," *J. Am. Ceram. Soc.*, **83** [3] 541–4 (2000).
[24]T. Takeuchi and H. Kageyama, "Preparation of $BaTiO_3/SrTiO_3$ Composite Dielectric Ceramics With a Flat Temperature Dependence of Permittivity," *J. Mater. Res.*, **18** [8] 1809–15 (2003).
[25]L. Zhou, Z. Zhao, A. Zimmermann, F. Aldinger, and M. Nygren, "Preparation and Properties of Lead Zirconate Stannate Titanate Sintered by Spark Plasma Sintering," *J. Am. Ceram. Soc.*, **87** [4] 606–11 (2004).
[26]B. Su, J. Y. He, B. L. Cheng, T. W. Button, J. Liu, Z. Shen, and M. Nygren, "Dielectric Properties of Spark Plasma Sintered (SPS) Barium Strontium Titanate (BST) Ceramics," *Integr. Ferroelectr.*, **61**, 117 –22 (2004).
[27]Z. Zhao, V. Buscaglia, M. Viviani, M. Buscaglia, L. Mitoseriu, A. Testino, M. Nygren, M. Johnsson, and P. Nanni, "Grain Size Effects on the Ferroelectric Behavior of Dense Nanocrystalline $BaTiO_3$ Ceramics," *Phys. Rev. B*, **70** [2] 024107 (2004).
[28]S. L. Swartz and T. R. Shrout, "Dielectric Properties of Lead Magnesium Niobate Ceramics," *J. Am. Ceram. Soc.*, **67** [5] 311–5 (1984).
[29]IEEE. *IEEE Standard on Piezoelectricity, ANSI/IEEE Standard No. 176*. IEEE, NY, 1987.
[30]K. Oonishi, T. Morohashi, and K. Uchino, "HIP Sintering of Fine Grained Barium Titanate," *J. Ceram. Soc. Jpn.*, **97** [4] 473–7 (1989).
[31]T. Takeuchi, M. Tabuchi, and H. Kageyama, "Preparation of Dense $BaTiO_3$ Ceramics with Submicrometer Grains by Spark Plasma Sintering," *J. Am. Ceram. Soc.*, **82** [4] 939–43 (1999).
[32]S. W. Choi, T. R. Shrout, S. J. Jang, and A. S. Bhalla, "Morphotropic Phase Boundary in $Pb(Mg_{1/3}Nb_{2/3})O_3$–$PbTiO_3$ System," *Mater. Lett.*, **8** [6–7] 253–5 (1989).
[33]B. Noheda, D. E. Cox, and G. Shirane, "Phase Diagram of the Ferroelectric Relaxor $(1-x)Pb(Mg_{1/3}Nb_{2/3})O_3-xPbTiO_3$," *Phys. Rev. B*, **66** [5] 054104 (2002).
[34]K. M. Lee, H. M. Jang, and W. J. Park, "Mechanism of 1:1 Nonstoichiometric Short-Range Ordering in La-Doped $Pb(Mg_{1/3}Nb_{2/3})O_3$ Relaxor Ferroelectrics," *J. Mater. Res.*, **12** [6] 1603–13 (1997).
[35]D. M. Fanning, I. K. Robinson, S. T. Jung, E. V. Colla, D. D. Viehland, and D. A. Payne, "Superstructure Ordering in Lanthanum-Doped Lead Magnesium Niobate," *J. Appl. Phys.*, **87** [6] 840–8 (2000).
[36]B. Vodopivec, C. Filipic, A. Levstik, J. Holc, Z. Kutnjak, and H. Beige, "Dielectric Properties of Partially Disordered Lanthanum-Modified Lead Zirconate Titanate Relaxor Ferroelectrics," *Phys. Rev. B*, **69** [22] 224208 (2004).
[37]K. Uchino, "High Electromechanical Coupling Piezoelectrics: Relaxer and Normal Ferroelectric Solid Solutions," *Solid State Ionics*, **108** [1–4] 43–52 (1998).
[38]G. S. Xu, H. S. Luo, H. Q. Xu, and Z. W. Yin, "Third Ferroelectric Phase in PMNT Single Crystals Near the Morphotropic Phase Boundary Composition," *Phy. Rev. B*, **64** [2] 020102 (2001).
[39]J. M. Kiat, Y. Uesu, B. Dkhil, M. Matsuda, C. Malibert, and G. Calvarin, "Monoclinic Structure of Unpoled Morphotropic High Piezoelectric PMN–PT and PZN–PT Compounds," *Phys. Rev. B*, **65** [2] 064106 (2002).
[40]L. Sun, Y. F. Chen, W. H. Ma, L. W. Wang, T. Yu, M. S. Zhang, and N. B. Ming, "Evidence of Ferroelectricity Weakening in the Polycrystalline $PbTiO_3$ Thin Films," *Appl. Phys. Lett.*, **68** [26] 3728–30 (1996).
[41]E. Nieto, J. F. Fernandez, C. Moure, and P. Duran, "Characterization of $Pb(Zr,Ti)O_3$ Thin Films Obtained by MOD," *J. Mater. Sci.*, **30** [24] 6243–8 (1995).
[42]Y. Park, E. J. Lee, and H. G. Kim, "Particle-Size-Induced Diffuse Phase Transition in the Fine-Particle Barium Titanate Porcelains," *J. Phys.: Condens. Matter*, **9**, 9445–56 (1997).
[43]X. H. Zhu, J. M. Zhu, S. Z. Zhou, Q. Li, Z. Y. Meng, Z. G. Liu, and N. B. Ming, "Domain Morphology Evolution Associated with the Relaxor-Normal Ferroelectric Transition in the Bi- and Zn-Modified $Pb(Ni_{1/3}Nb_{2/3})O_3$–$PbZrO_3$–$PbTiO_3$ System," *J. Euro. Ceram. Soc.*, **20**, 1251–5 (2000).
[44]J. Carreaud, P. Germeiner, J. M. Kiat, B. Dkhil, C. Bogicevic, T. Rojac, and B. Malic, "Size-Driven Relaxation and Polar States in $Pb(Mg_{1/3}Nb_{2/3})O_3$-Based System," *Phys. Rev. B*, **72**, 174115 (2005).
[45]B. P. Zhang, L. M. Zhang, J. F. Li, J. L. Zhang, and S. Z. Jin, "SPS Sintering of $NaNbO_3$–$KNbO_3$ Piezoelectric Ceramics," *Mater. Sci. Forum*, **475–479**, 1165–8 (2005).
[46]R. P. Wang, R. J. Xie, T. Sekiya, and Y. Shimojo, "Fabrication and Characterization of Potassium–Sodium Niobate Piezoelectric Ceramics by Spark-Plasma-Sintering Method," *Mater. Res. Bull.*, **39** [11] 1709–15 (2004). □